

⁷R. S. Hughes, G. E. Everett, and A. W. Lawson,
Phys. Rev. B **9**, 2394 (1974).

⁸B. Lax and K. J. Button, *Microwave Ferrites and*

Ferrimagnetics (McGraw-Hill, New York, 1962).

⁹C. Demangeat, D. L. Mills, and S. E. Trullinger,
Phys. Rev. B **16**, 522 (1977).

Electronic Structure of Semiconducting Films upon Ordering, as Observed by Double-Beam Photoemission

L. D. Laude, M. Lovato, M. C. Martin, and M. Wautelet
Université de l'Etat, B-7000 Mons, Belgium

(Received 27 June 1977)

The evolution of the electronic structure of disordered Te and Ge films upon thermal annealing and/or laser irradiation has been traced with use of the newly developed double-beam photoemission technique. In particular, it is shown that, contrary to what occurs in Te films, the onset of short-range crystalline ordering appears abruptly and uniformly within the Ge films, but over a much too short range to avoid \vec{k} randomization before emission of the electrons.

The field of disordered solids is generally recognized as a puzzling one. However, among the positive information collected so far, atomic distribution studies have shown that crystalline short-range order is more or less present in disordered films. In parallel, photoemission has indicated that the structure of the crystalline valence-band density of states (DOS) would seem generally to be much less affected by the absence of long-range order in the disordered films than the conduction-band DOS.

Upon thermal annealing, as the atomic configuration evolves towards the crystal with increasing temperature, the electronic structure of the films, as seen by photoemission, resembles more and more that of the crystal. However, because of the limited resolution of photoemission, it was never possible to identify clearly any inter-

mediate phase in that evolution. It was the purpose of the present work to investigate such ordering mechanisms developing in disordered semiconducting films (namely Ge and Te) upon thermal annealing and/or laser irradiation. It has been shown recently¹ that the possibility exists to modulate the photoemission current of a solid by using a flash-excited dye-laser (secondary) beam focused onto the sample together with the continuous uv (primary) beam. This double-beam photoemission technique (DBP) has proved to provide extremely precise information on the electronic structure of crystals.

Following arguments developed earlier,¹ DBP may be regarded as a two-step optical process via *real* intermediate conduction states. In the case of a crystal, the resulting DBP electron distributions can be expressed by

$$\begin{aligned}
 N(E, h\nu_{uv}, h\nu_L) = & \sum_{\vec{k}} P(E, \vec{k}) | \langle M_{VC_1}(\vec{k}) \rangle |^2 \delta(E_V(\vec{k}) + h\nu_L - E_{C_1}(\vec{k})) \\
 & \times [| \langle M_{C_1C_3}(\vec{k}) \rangle |^2 \delta(E_{C_1}(\vec{k}) + h\nu_{uv} - E_{C_3}(\vec{k})) \delta(E - E_{C_3}(\vec{k})) \\
 & + | \langle M_{VC_2}(\vec{k}) \rangle |^2 \delta(E_V(\vec{k}) + h\nu_{uv} - E_{C_2}(\vec{k})) \delta(E - E_{C_2}(\vec{k}))], \quad (1)
 \end{aligned}$$

where V and C label electron-state energy levels in the valence and conduction bands, respectively, $P(E, \vec{k})$ is the usual escape function of excited electrons, and M denotes the various matrix elements involved, with the summation running over the whole Brillouin zone.

The first term on the right-hand side of Eq. (1) describes the pulsed laser excitation of valence electrons into conduction states, followed by the uv excitation of these once-excited electrons into higher conduction states (process 1, in Ref. 1); the second term represents the uv excitation of valence electrons the density of which has been modulated through laser excitation (process 2, in Ref. 1).² In the absence of periodicity, \vec{k} conservation does not hold and Eq. (1) may be reduced to two distributions

given by

$$N_1^*(E, h\nu_{uv}, h\nu_L) = P(E) | \langle M_{VC_1}(h\nu_L) \rangle |^2 | \langle M_{C_1C_3}(h\nu_{uv}) \rangle |^2 n(E - h\nu_{uv} - h\nu_L) n(E - h\nu_{uv}) n(E) \quad (2a)$$

for $E > h\nu_{uv}$,

$$N_2^*(E, h\nu_{uv}, h\nu_L) = P(E) | \langle M_{VC_1}(h\nu_L) \rangle |^2 | \langle M_{VC_2}(h\nu_{uv}) \rangle |^2 n(E - h\nu_{uv}) n(E - h\nu_{uv} + h\nu_L) n(E) \quad (2b)$$

for $E \leq h\nu_{uv}$,

where the $\langle M \rangle$'s are \bar{k} -averaged matrix elements coupling level E with lower-energy levels E' such that $E - E' = h\nu_L$ or $h\nu_{uv}$; the n 's are DOS values at particular energy levels; and $P(E)$ is a \bar{k} -averaged escape function.

Films were prepared in 2×10^{-10} -Torr vacuum, by thermal evaporation and subsequent condensation on glass substrates maintained at -40°C or $+20^\circ\text{C}$ for Te, and 20°C for Ge. Annealing was performed by heating or laser irradiation.³ Only some of the most characteristic DBP spectra are presented in this Letter. Details of the DBP set-up have been given elsewhere.¹

Spectra obtained from Te films at uv energy $h\nu_{uv} = 7.71$ eV and laser energy $h\nu_L = 4.16$ eV are shown in Fig. 1. They are compared to a Te (10 $\bar{1}0$) spectrum (dashed line) measured under the same irradiation conditions. Curve a_1 refers to a Te film deposited and maintained at -40°C during measurement; curve b_1 , to a film deposited at 20°C ; curve c_1 , to a film deposited at 20°C , annealed at 110°C , and cooled at 20°C ; curve d_1 , as in c_1 but, in addition, laser irradiated for several hours at $h\nu_L = 2.08$ eV. Attention is focused essentially on the forbidden gap existing in the conduction-band DOS of trigonal Te,¹ between 2.5 and 4.7 eV above valence-band edge (VBE) as seen in curve d_2 . The absence of states in that energy range is demonstrated experimentally by the location of *both* the upper limits of the high- and low-energy parts of the spectrum d_1 , at $E = 10.2$ eV ($= 2.5 + 7.7$ eV) and 6.0 eV ($= 2.5 - 4.16 + 7.7$ eV), respectively. The lower limit of d_1 delineates the bottom of the second (d -like) conduction band in trigonal Te.

In the film spectra a_1 and b_1 , the low-energy onset of the spectra at $E = 4.2$ eV (photoelectric threshold of these Te films) indicates that energy levels do exist at $E > 4.2$ eV. In addition, the upper limits of the low- and high-energy parts of these spectra, at $E = 7.7$ and $7.7 + 4.16 \approx 11.9$ eV demonstrate the presence of conduction states up to ~ 4.2 eV above VBE, i.e., there exists no for-

bidden gap *at all* within the conduction band of Te films deposited and maintained at temperatures below or equal to 20°C . This behavior is in good agreement with a previous model calculation of the electronic structure of disordered Te,⁴ which predicted the disappearance of the p_3 - d gap in disordered Te. Furthermore, the profile of the corresponding DBP spectra at below $E = 7.7$ eV corresponds almost exactly to the calculated valence-band DOS of trigonal Te,⁵ d_2 , except for a minor difference between a_1 and b_1 around $E = 6$ eV (initial-states energy level at 1.7 eV below VBE). The low-energy part of a_1 or b_1 at $E < 7.7$ eV is nearly identical to classical photoemission (PE) spectra obtained at $h\nu_{uv} = 7.71$ eV from iden-

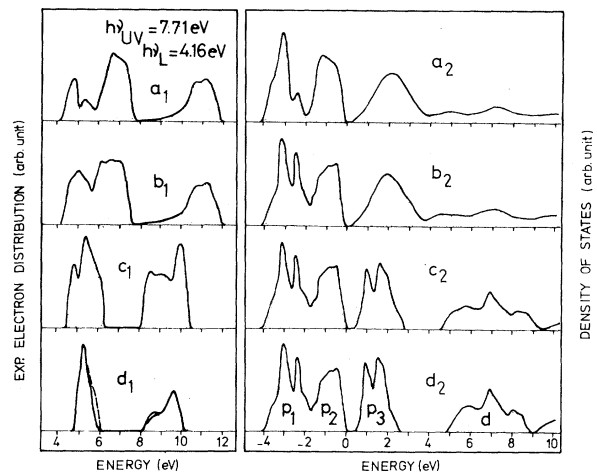


FIG. 1. DBP spectra (left-hand side) and corresponding densities of states (right-hand side) of Te films (solid lines) and (10 $\bar{1}0$) Te (dashed line). Energy zero is at valence-band edge. Crystalline DOS is shown in d_2 (Ref. 5). Spectrum d_1 is well reproduced from Eq. (1) with use of this DOS. Curve c_2 is a broadened version of d_2 , where the respective limits of the p_3 and d bands have been adjusted to fit spectrum c_1 (see text). The DOS shown in a_2 and b_2 were deconvoluted from spectra a_1 and b_1 , respectively, with use of Eqs. (2) and (3).

tically prepared Te films.⁶ These PE spectra have been shown to be very similar to the one obtained from Te (10 $\bar{1}$ 0). DBP decisively allows a clear distinction to be drawn between these materials.

The following procedure has been adopted to describe the measured disordered Te spectra:

(a) Without \vec{k} conservation, the imaginary part of the dielectric constant, ϵ_2 , reduces to

$$\epsilon_2(h\nu) = |\langle\langle M(h\nu) \rangle\rangle|^2 n_v(E - h\nu) n_c(E), \quad (3)$$

where $\langle\langle M(h\nu) \rangle\rangle$ are energy- and \vec{k} -averaged matrix elements; $n_v(E - h\nu)$ and $n_c(E)$, the valence- and conduction-band DOS, respectively. This model is applied to the crystal case and yields $\langle\langle M(h\nu) \rangle\rangle$. It is then extended to the disordered case by energy broadening identically $n_c(E)$ and $\langle\langle M(h\nu) \rangle\rangle$ to fit ϵ_2 , which has been independently measured from similarly prepared Te disordered films.⁷ This gives $n_c(E)$ which is used in Eq. (2).

(b) A comparison of processes 1 and 2 within the *same* DBP spectrum measured at a given $h\nu_{uv}$ value provides the energy profile of $\langle M_{VC_2} \rangle$ relative to $\langle M_{C_1C_3} \rangle$ which may be taken to be constant.

(c) Finally, a fit of Eq. (2) to the DBP spectrum measured at $h\nu_{uv}$ is achieved by adjusting $\langle M_{VC_1} \rangle$. All other DBP spectra are then calculated and checked to duplicate experimental data. Results of this deconvolution procedure are given in Fig. 1, curves a_2 and b_2 . Upon annealing it is remarkable to note that the evolution towards the trigonal electronic structure is a *progressive* one. In Fig. 1, curve c_2 , the *p-d* gap opens up from $E = 2.8$ to 4.5 eV and the upper limit of the *d* band is at $E = 9.5$ eV. After extended laser irradiation, the film duplicates the crystalline spectrum, Fig. 1, curve d_1 . It is obvious that spectrum c_1 is not an approximate average of spectra b_1 and d_1 . Note that the film annealed at 110°C (c_1) would appear to be very roughly crystallized by x-ray-diffraction means.⁸

DBP spectra obtained at $h\nu = 5.75$ eV and $h\nu_L = 4.16$ eV from Ge films deposited at 20°C are shown in Fig. 2. After laser irradiation over 7 h at $h\nu_L = 2.08$ eV, spectra evolve from a_1 (measured right after deposition), through b_1 and c_1 , into d_1 which corresponds fairly well to the crystal spectrum (dashed line). In b_1 ,⁹ the low-energy peak of a_1 is still present¹⁰ but the two broad peaks centered at $E = 7.9$ and 9.0 eV in a_1 give room to an asymmetric profile having a sharp leading edge above $E = 6.5$ eV followed by a monotonous decrease up to $E = 9.9$ eV. In c_1 , the low-energy peak is absent and two structures seem

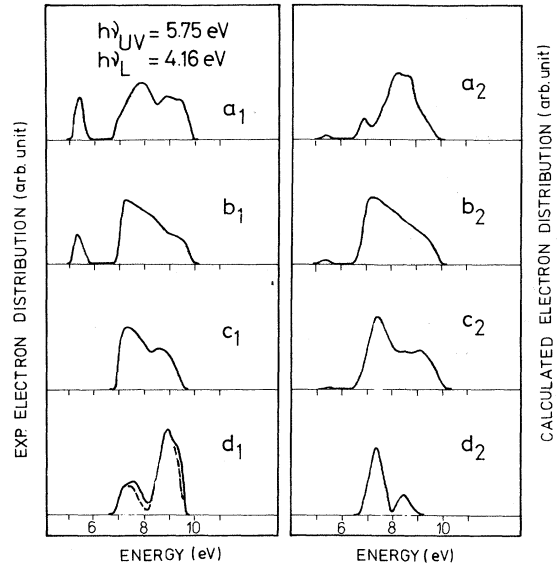


FIG. 2. Experimental (left-hand side) and theoretical (right-hand side) DBP spectra of Ge films. Energy zero is at the valence-band edge. Theoretical spectra were obtained according to models described in text. Curve c_2 is averaged between b_2 and d_2 and compares well with c_1 .

to be superimposed onto the preceding profile, b_1 . The last step of the evolution in d_1 leads to a typically crystalline spectrum (dashed line).

Model calculations of DBP spectra have been carried out for Ge using constant matrix elements and (a) a broadened version of the crystal DOS of Ge⁴ assuming only energy conservation [Eq. (2)]; (b) the true crystal DOS,¹¹ again assuming no \vec{k} conservation [Eq. (2)]; (c) the crystal DOS,¹¹ with both energy and \vec{k} conservations [Eq. (1)]. Results are shown in Fig. 2, curves a_2 , b_2 , and d_2 , respectively. The first model, a_2 , fails to recover the measured spectrum, a_1 , although the same model was able to describe well spectra of Fig. 1, curves a_1 and b_2 , measured from disordered Te films. The second model (the so-called non-direct-transition model¹²) is shown to reproduce almost perfectly the intermediate spectrum b_1 . The third model yields the two peaks of d_1 , the difference in intensities being ascribed to matrix elements effects¹³ [Eq. (1)]. The noticeable feature in this evolution is the occurrence of spectrum b_1 which, by comparison with b_2 , may be regarded as the very first indication of ordering in the Ge films. In contrast with the Te films, crystalline ordering appears *abruptly* and uniformly in the Ge films: In Fig. 2, curve b_1 has absolutely nothing in common with curve a_1

at $E > 6.5$ eV. At this stage, however, ordering is strongly shadowed by (a) elastic scattering resulting in \vec{k} relaxation (see process 1, Fig. 2, curve b_1), and (b) possibly inelastic scattering which would explain the relatively higher intensity or process-2 contribution in b_1 compared to the same energy range in b_2 .¹⁴ On the other hand, curve c_1 can be easily reconstructed from an average between curves b_1 and d_1 , just like curve c_2 which is the average of curves b_2 and d_2 .

From this comparison between experimental DBP spectra (Fig. 2, left-hand side) and spectra calculated from Eqs. (1) and (2) (Fig. 2, right-hand side), one might conclude that, although the emergence of diamondlike ordering in Ge films is uniform and abrupt, it appears first over a much too short range to avoid \vec{k} randomization before emission of the electrons. This ordering develops further in a nonuniform manner within the Ge films until full crystallization is achieved.

In this work, a rather precise picture of the DOS profile both in the valence and conduction bands of disordered semiconducting films is revealed with use of the DBP technique. Furthermore, it is shown that laser irradiation might prove to be an extremely powerful method of inducing precise ordering in semiconductors, while at room temperature. This would appear potentially valuable, particularly for high-vapor-pressure materials. In addition, this laser-induced ordering, developing progressively over extended periods of time, offers the possibility to explore the kinematics of ordering processes in the technology of semiconductors. A detailed presentation of this work will be published elsewhere.

This work was supported by project IRIS of the

Belgian Ministry for Science Policy.

¹M. Wautelet and L. D. Laude, Phys. Rev. Lett. **38**, 40 (1977); L. D. Laude and M. Wautelet, Nuovo Cimento **39B**, 734 (1977).

²Other possible processes, like the uv (followed by the laser) excitations of valence electrons or typical two-photon processes (via virtual states) have been shown not to contribute DBP spectra in trigonal Te (Ref. 1), and are not presently taken into consideration in Eq. (1).

³Because of the short pulse duration of the laser (10^{-6} s; repetition rate is 16.7 Hz), the temperature of the film remained effectively constant at 20°C.

⁴B. Kramer, Phys. Status Solidi **49**, 525 (1972).

⁵K. Maschke, Phys. Status Solidi **47**, 511 (1971).

⁶L. D. Laude, B. Kramer, and K. Maschke, Phys. Rev. B **8**, 5794 (1973).

⁷N. Didden, Z. Phys. **257**, 310 (1972).

⁸M. J. Caspers and M. White, Thin Solid Films **8**, 353 (1971).

⁹Identical spectra are obtained after thermal annealing of the films at 200°C.

¹⁰Ordinary PE spectra of disordered Ge films and Ge crystal measured at $h\nu_{uv} = 5.7$ eV are exactly identical. In addition, these spectra are quite comparable to the low-energy peak of Fig. 2, curve a_1 or b_1 , at $E > 5.7$ eV. Then it is not surprising at all that the intermediate phase which yields Fig. 2, curve b_1 could not be evidenced on PE spectra.

¹¹W. D. Grobman, D. E. Eastman, and J. L. Freeouf, Phys. Rev. B **12**, 4405 (1975).

¹²W. E. Spicer, Phys. Rev. **154**, 385 (1967).

¹³L. D. Laude and M. Wautelet, to be published.

¹⁴An alternative explanation would be an effective higher density of states near the top of the valence band in amorphous Ge compared to crystalline Ge, associated with bond-angle fluctuations in the disordered material (J. D. Joannopoulos, Phys. Rev. B **16**, 2764 (1977)).